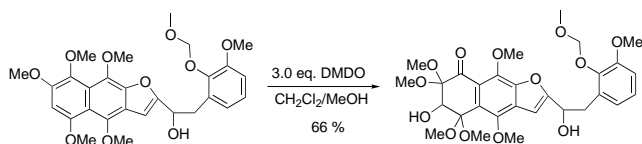


Scheme 8. Reagents and conditions: a)  $\text{BBr}_3$  (15 equiv),  $\text{CH}_2\text{Cl}_2$ ,  $-78^\circ\text{C}$ , 52%; b)  $\text{HCl}$  (1N, 100 equiv),  $65^\circ\text{C}$ , THF, quantitative.

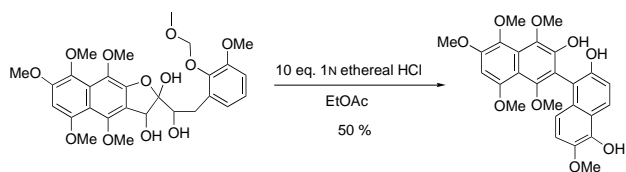
Our longer term goals in the project involve an enantiodefined synthesis of **2**, a synthesis of heliquinomycin itself, and an evaluation of the *anti* helicase activity of the various heliquinomycin analogues that were formed in the project. It is expected that the identification of the complexities of the problem described herein and the synthesis of the aglycone portion, will be of benefit in future synthetic projects.

Received: September 5, 2001 [Z17860]

- [1] D. Qin, R. X. Ren, T. Siu, C. Zheng, S. J. Danishefsky, *Angew. Chem.* **2001**, *113*, 4845; *Angew. Chem. Int. Ed.* **2001**, *40*, 4709.  
 [2] An interesting example of the problems associated with the electron richness of the naphthalene ring in hindering the desired epoxidation of the furan is shown in a model substrate:



- [3] a) S. Tang, R. M. Kennedy, *Tetrahedron. Lett.* **1992**, *33*, 5303; b) R. M. Kennedy, S. Tang, *Tetrahedron Lett.* **1992**, *33*, 3729.  
 [4] For previous examples of dihydroxylations of benzofuran and indole rings, see: a) M. P. Meisinger, F. A. Kuehl, Jr., E. L. Rickes, N. G. Brink, K. Folkers, M. Forbes, F. Zilliken, P. Gyorgy, *J. Am. Chem. Soc.* **1959**, *81*, 4979; b) G. B. Feigelson, M. Egbertson, S. J. Danishefsky, *J. Org. Chem.* **1988**, *53*, 3390.  
 [5] A demonstration of the vulnerability of the C3' position even relative to C2 in a model substrate is shown below:



- [6] O. Mitsunobu, *Synthesis* **1981**, 1.  
 [7] H. Ishii, T. Ishikawa, S. Takeda, S. Ueki, M. Suzuki, *Chem. Pharm. Bull.* **1992**, *40*, 1148.

- [8] Hydride reduction of protected variants of **11** and **12** that contained bulky protecting groups on the C3 hydroxy function also gave only products **13** and **14**.  
 [9] Both diastereomers show clear NOE enhancements between the C3 methine and the C3' methine. No NOE interaction was observed between these two protons in heliquinomycin.  
 [10] The results of this reaction support a mechanism for epimerization at C3' rather than the more traditional epimerization at C2 of the spiro center. Had epimerization at C2 occurred, the product of **12** would have corresponded to either one of the products derived from **11**. No such crossover was observed.  
 [11] The C4 protons of **16** appear as a doublet whereas the C4 protons of naturally derived heliquinomycinone appear as two doublets of doublets.  
 [12] H. C. Kolb, M. S. van Nieuwenhze, K. B. Sharpless, *Chem. Rev.* **1994**, *94*, 2483.

## Heat Capacity of the Mixed-Valence Complex $\{[(n\text{-C}_3\text{H}_7)_4\text{N}][\text{Fe}^{\text{II}}\text{Fe}^{\text{III}}(\text{dto})_3]\}_\infty$ , Phase Transition because of Electron Transfer, and a Change in Spin-State of the Whole System\*\*

Tadahiro Nakamoto, Yuji Miyazaki, Miho Itoi, Yuuki Ono, Norimichi Kojima,\* and Michio Sorai\*

Recently a novel mixed-valence complex  $\{[(n\text{-C}_3\text{H}_7)_4\text{N}][\text{Fe}^{\text{II}}\text{Fe}^{\text{III}}(\text{dto})_3]\}_\infty$  (**1**) containing asymmetric ligand dto (dithiooxalato:  $\text{C}_2\text{O}_2\text{S}_2^{2-}$ ) was synthesized by Kojima and co-workers.<sup>[1]</sup> This complex displays ferromagnetic order below  $\sim 6$  K and exhibits an interesting phenomenon at temperatures between 110 K and 120 K, where a change in the spin state of the whole system occurs as the result of electron transfer. This situation is schematically shown in Figure 1.

[\*] Prof. Dr. M. Sorai, Dr. Y. Miyazaki, Dr. T. Nakamoto  
 Research Center for Molecular Thermodynamics  
 Graduate School of Science, Osaka University  
 Toyonaka, Osaka 560-0043 (Japan)  
 Fax: (+81) 6-6850-5526  
 E-mail: sorai@chem.sci.osaka-u.ac.jp  
 Prof. Dr. N. Kojima, M. Itoi, Y. Ono  
 Graduate School of Arts and Science  
 The University of Tokyo  
 Komaba, Tokyo 153-8902 (Japan)  
 Fax: (+81) 3-5454-4311  
 E-mail: cnori@mail.ecc.u-tokyo.ac.jp

[\*\*] Contribution No. 48 from the Research Center for Molecular Thermodynamics. This work was partially supported by a Grant-in-Aid for Scientific Research on the Priority Areas of "Metal-Assembled Complexes" (Area No. 401/12023229) from the Ministry of Education, Science, Sports and Culture, Japan; dto = dithiooxalato.

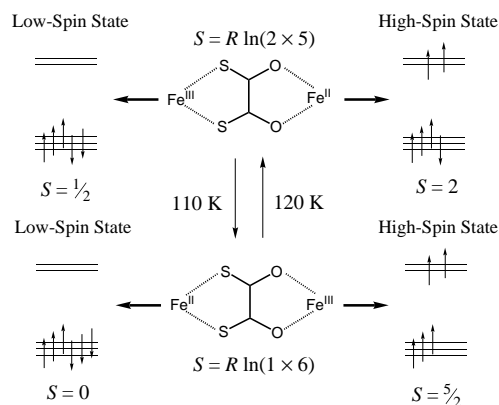


Figure 1. Schematic representation of the electron transfer phenomenon in  $\{(n\text{-C}_3\text{H}_7)_4\text{N}[\text{Fe}^{\text{II}}\text{Fe}^{\text{III}}(\text{dto})_3]\}_\infty$ . Symbol  $S$  has been used both for the spin quantum number (left and right) and for the entropy arising from the spin multiplicity (center).

Although the structure of the complex has not been determined owing to the lack of suitable single crystals, at room temperature a network structure with an alternating array of  $\text{Fe}^{\text{II}}$  and  $\text{Fe}^{\text{III}}$  ions bridged by dto ligands bonding through the S atoms to  $\text{Fe}^{\text{III}}$  centers and through O atoms to the  $\text{Fe}^{\text{II}}$  centers may be presumed by analogy to bimetallic oxalato complexes.<sup>[2]</sup> The coordination spheres of both Fe sites are presumed to be twisted trigonal prismatic also by analogy of other dto complexes.<sup>[3]</sup> The valence and the spin states of each Fe site were determined by  $^{57}\text{Fe}$  Mössbauer spectroscopy.<sup>[1]</sup> At 200 K the  $\text{FeO}_6$  site is divalent and in a high-spin (HS) state ( $^5\text{T}_{2g}$ ,  $S = 2$ ;  $S$  = spin quantum number), while the  $\text{FeS}_6$  site is trivalent and in a low-spin (LS) state ( $^2\text{T}_{2g}$ ,  $S = 1/2$ ). At 77 K, however, as a result of the electron transfer, the  $\text{FeO}_6$  site becomes trivalent and is in an HS state ( $^6\text{A}_{1g}$ ,  $S = 5/2$ ) while the  $\text{FeS}_6$  site is converted to divalent state and in an LS state ( $^1\text{A}_{1g}$ ,  $S = 0$ ). On the basis of the magnetic-susceptibility measurement the transition temperature between these two states was determined to be 110 K on cooling and 120 K on heating.<sup>[4]</sup>

At first glance, this phenomenon seems to be a type of spin crossover because a change in the spin state actually occurs in the whole system. However, there is a crucial difference between this phenomenon and usual spin-crossover phenomenon. No spin crossover has been reported for  $\text{FeO}_6$  complexes regardless of the valence state of the Fe center, while several spin-crossover  $\text{FeS}_6$  complexes have been found in ferric compounds such as tris(dithiocarbamate) complexes  $[\text{Fe}^{\text{III}}(\text{dtc})_3]$ .<sup>[5]</sup> In the title complex, however, since the  $\text{Fe}^{\text{III}}$  ion in  $\text{FeS}_6$  site is already in the LS state at room temperature, temperature-induced spin-crossover phenomenon can no longer be expected at low temperatures. Therefore, neither of two Fe sites can independently cause a temperature-induced spin-crossover phenomenon. Although a great number of spin-crossover systems<sup>[6–8]</sup> and mixed-valence systems<sup>[9–10]</sup> are known, a system such as **1** is unknown. Investigation of thermal properties provides us with important information concerning energy and entropy. To shed light on this phenomenon from a thermodynamic viewpoint, we measured heat capacities of **1**. Herein we describe the mechanism of the novel electron transfer transition.

Observed molar heat capacities under constant pressure ( $C_p$ ) of  $\{(n\text{-C}_3\text{H}_7)_4\text{N}[\text{Fe}^{\text{II}}\text{Fe}^{\text{III}}(\text{dto})_3]\}_\infty$  are plotted in Figure 2. A sharp peak at 122.4 K and a broad heat-capacity anomaly centered at 253.5 K are observed. The origin of the latter heat

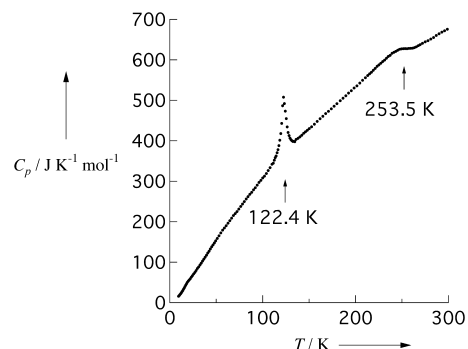


Figure 2. Molar heat capacity of crystalline  $\{(n\text{-C}_3\text{H}_7)_4\text{N}[\text{Fe}^{\text{II}}\text{Fe}^{\text{III}}(\text{dto})_3]\}_\infty$  as a function of temperature.

capacity anomaly can be attributed to an order–disorder type of phase transition of  $[(n\text{-C}_3\text{H}_7)_4\text{N}]^+$  ion, based on similar heat-capacity anomalies observed in the analogous molecule-based magnets such as  $\{(n\text{-C}_4\text{H}_9)_4\text{N}[\text{M}^{\text{II}}\text{Fe}^{\text{III}}(\text{ox})_3]\}_\infty$  where  $\text{M} = \text{Fe}$  or  $\text{Zn}$ .<sup>[13]</sup> The anomaly at 122.4 K clearly arises from the phase transition resulting from the electron transfer, as the transition temperature agrees well with the temperature at which the anomaly was observed in the magnetic-susceptibility measurements.<sup>[4]</sup>

In addition, a small heat capacity hump was observed around 20 K. As no event has been found in this temperature region by the magnetic-susceptibility measurement, the origin of this anomaly has not been assigned. The very low-temperature heat capacity of **1** measured by use of a calorimeter with a  $^3\text{He}/^4\text{He}$  dilution refrigerator, will be reported, in due course, along with the magnetic heat capacity arising from the ferromagnetic transition at  $\sim 6\text{ K}$ <sup>[4]</sup> together with the analysis of the heat-capacity anomaly observed around 20 K.

Although the phase transition at 122.4 K does not take place isothermally, it should be regarded as first-order phase transition, because supercooling phenomenon have been observed. As shown in Figure 3a, no anomaly was detected in the measurement for the specimen cooled to 110 K. Two small  $C_p$  waves, seen in the 120–130 K region, were caused by the experimental condition that we adopted, that is, the rather small temperature increment for  $C_p$  determination. The sample cooled to 100 K exhibited a small anomaly. This anomaly became larger as the temperature was lowered. This observation indicates that the transition temperature upon cooling  $T_c(\downarrow)$  is about 110 K, which is in good agreement with the  $T_c(\downarrow)$  determined by the magnetic-susceptibility measurement.<sup>[4]</sup>

For determination of the excess heat capacities because of the electron-transfer phenomenon, it is necessary to estimate a normal heat capacity or lattice heat capacity,  $C_{\text{lat}}$ . For this purpose the effective frequency distribution method<sup>[14]</sup> is a good approximation. In the present case, however, this procedure seems to be difficult because of the presence of the broad heat capacity anomaly centered at 253.5 K, the starting temperature of which is difficult to determine. In the

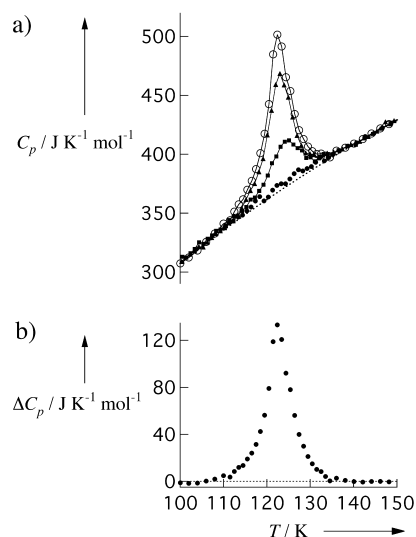


Figure 3. a) Molar heat capacities of crystalline  $[(n\text{-C}_5\text{H}_7)_4\text{N}][\text{Fe}^{\text{II}}\text{Fe}^{\text{III}}(\text{dto})_3]_\infty$  in the vicinity of the phase transition at 122.4 K. ( $\circ$ ) are the data shown in Figure 2, which correspond to the heat capacities for the specimen well annealed at 100 K after once cooled to 80 K and then cooled again to 5 K. Filled symbols indicate the data obtained after cooling to the temperatures: ( $\bullet$ ) 110 K, ( $\blacksquare$ ) 100 K, and ( $\blacktriangle$ ) 90 K. The solid curves are to aid the eye. The dashed curve shows for the normal heat capacity. b) Excess molar heat capacities because of the phase transition.

present complex, however, the  $C_p$  data of the supercooling state seems to coincide well with those of the low-temperature phase below  $T_c$ . Therefore the  $C_{\text{lat}}$  curve was estimated by a least-squares fitting of a polynomial function of temperature,  $aT^2 + bT + c$ , to the  $C_p$  data in the temperature range between 80 K and 160 K. The “best fit”  $C_{\text{lat}}$  curve thus determined is represented by Equation (1) and shown in Figure 3a by dashed curve.

$$C_{\text{lat}} [\text{J K}^{-1} \text{mol}^{-1}] = -67.81 + 4.657 T [\text{K}] - 0.008935 (T [\text{K}])^2 \quad (1)$$

(80 < T [K] < 160)

The difference between the observed and the normal heat capacities shown in Figure 3b corresponds to the excess heat capacity,  $\Delta C_p$ . The enthalpy and entropy arising from the electron-transfer phenomenon are determined to be  $\Delta_{\text{trs}}H = 1.04 \text{ kJ mol}^{-1}$  and  $\Delta_{\text{trs}}S = 9.20 \text{ J K}^{-1} \text{mol}^{-1}$ , respectively.

The entropy change is larger than the spin-only value expected for the change in the spin multiplicity  $R\ln(10/6) = 4.25 \text{ J K}^{-1} \text{mol}^{-1}$ . Should the ligand-field symmetry remain  $O_h$  through out the phase transition, then the change in the orbital angular momentum contributes  $R\ln[(3 \times 3)/(1 \times 1)] = 18.27 \text{ J K}^{-1} \text{mol}^{-1}$  to the entropy gain. If this is the case, the total entropy gain because of the spin and orbital amounts to  $22.51 \text{ J K}^{-1} \text{mol}^{-1}$ . However, this is not the case because this value is far beyond the experimental entropy. The orbital degeneracy, such as  $^5T_{2g}$  and  $^2T_{2g}$  encountered in high-spin  $\text{Fe}^{\text{II}}$  and low-spin  $\text{Fe}^{\text{III}}$  systems in an  $O_h$  symmetry, is usually lifted by the Jahn–Teller distortion to give a nondegenerate or lower-degenerate ground state. In such a case, the orbital contribution to the entropy becomes small or negligible. In **1**, it is very likely that a trigonal distortion is encountered in the  $\text{FeO}_6$  and  $\text{FeS}_6$  sites. Under such a situation, the ground terms

$^5T_{2g}$  of  $\text{Fe}^{\text{II}}(\text{HS})$  and  $^2T_{2g}$  of  $\text{Fe}^{\text{III}}(\text{LS})$  in  $O_h$  ligand-filled symmetry are reduced to  $^5E$  and  $^2A$  in a trigonal symmetry,<sup>[15]</sup> respectively. If this orbital contribution is fully taken into account, the electronic entropy gain from spin and orbital will be  $R\ln[(10 \times 2)/6] = 10.01 \text{ J K}^{-1} \text{mol}^{-1}$ . This value is very close to the experimental value of  $9.20 \text{ J K}^{-1} \text{mol}^{-1}$  resulting from the electron-transfer phenomenon. Although we discussed the orbital contribution to entropy for octahedral and trigonal ligand fields, there is a possibility that the actual ligand-field symmetry of **1** is lower than trigonal symmetry. In such a case, the orbital contribution to the entropy gain is further reduced. Therefore, the entropy gain expected from the electron transfer is in the range between  $R\ln(10/6) = 4.25 \text{ J K}^{-1} \text{mol}^{-1}$  from the spin multiplicity and  $R\ln(20/6) = 10.01 \text{ J K}^{-1} \text{mol}^{-1}$  from the spin and the orbital in trigonal symmetry.

Since the observed entropy gain is  $9.20 \text{ J K}^{-1} \text{mol}^{-1}$ , the entropy originating in intramolecular vibrations is considerably smaller than in normal spin-crossover phenomena. For example, about  $35 \text{ J K}^{-1} \text{mol}^{-1}$  was estimated for the vibrational contribution to the entropy change in the spin-crossover phenomenon observed in  $[\text{Fe}(\text{phen})_2(\text{NCS})_2]^{[16]}$  and  $37 \text{ J K}^{-1} \text{mol}^{-1}$  for  $[\text{Fe}(\text{2-pic})_3]\text{Cl}_2 \cdot \text{EtOH}$ .<sup>[17]</sup>

The magnitude of vibrational entropy crucially depends on the bond lengths between the metal ion and the ligands. The longer the bond length, the greater the vibrational entropy is. The metal–ligand bond length is affected by the spin state of the metal ion: it is longer for the HS state than for the LS state. Therefore, the normal spin-crossover phenomenon always involves a large entropy gain from the metal–ligand skeletal vibrations. In **1**, the  $\text{FeO}_6$  site is in the HS state and the  $\text{FeS}_6$  site is in the LS state, irrespective of the oxidation state. Therefore, in a strict sense both the Fe sites do not experience the spin-state conversion encountered in normal spin-crossover phenomena. However, since the oxidation states at the  $\text{FeO}_6$  and  $\text{FeS}_6$  sites are altered by the electron transfer, one can expect a change in vibrational system.

Another factor determining the bond length is the oxidation state of the metal ion. According to Shannon,<sup>[18]</sup> typical ionic radii of low-spin Fe ions with coordination number six are 75 pm and 69 pm for  $\text{Fe}^{\text{II}}(\text{LS})$  and  $\text{Fe}^{\text{III}}(\text{LS})$ , respectively. As shown in Figure 4, the metal–ligand bond lengths are elongated by 13.5 pm at the  $\text{FeO}_6$  site at the phase transition while those at the  $\text{FeS}_6$  site contract by 6 pm. When the phase transition as a result of the electron transfer occurs, the  $\text{FeO}_6$  site remarkably contributes positively to the vibrational entropy whereas the  $\text{FeS}_6$  site has a negative contribution. If the oxidation and reduction sites consisted of identical ligands, these two conflicting contributions to entropy would be canceled out and thus no vibrational entropy would be expected. In the present case, however, since the ligands are not identical and the relative atomic masses are different (O: 15.9994, S: 32.065), a net, though very small, contribution to the vibrational entropy is expected. To confirm experimentally the vibrational contribution to the entropy gain, variable-temperature IR spectroscopy investigations are now in progress.

In the mixed-valence complex **1** the spin state of the whole system dramatically changes by virtue of the electron transfer. At first glance, this phenomenon seems to be a type of spin-

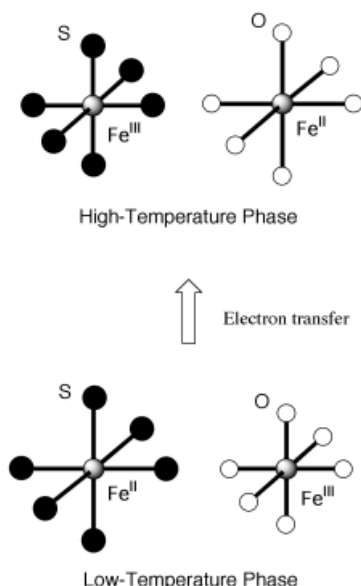


Figure 4. The relationship between the electron transfer and the metal–ligand bond lengths.

crossover phenomenon. However, the present calorimetric study clearly revealed that this novel phenomenon is quite different from usual (or classical) spin-crossover phenomenon.

#### Experimental Section

Synthesis of **1** is reported elsewhere.<sup>[1, 4]</sup> Heat capacity measurements between 8 K and 300 K were made with a home-built adiabatic microcalorimeter.<sup>[11, 12]</sup> The mass of the sample for calorimetry was 0.95853 g (1.4556 mmol). A small amount of He gas was sealed in the calorimeter cell to aid the heat transfer.

Received: May 21, 2001

Revised: August 27, 2001 [Z17145]

- [1] N. Kojima, W. Aoki, M. Seto, Y. Kobayashi, Yu. Maeda, *Synth. Met.* **2001**, *121*, 1796–1797.
- [2] S. Decurtins, H. W. Schmalke, H. R. Oswald, A. Linden, J. Ensling, P. Gütlich, A. Hauser, *Inorg. Chim. Acta* **1994**, *216*, 65–73.
- [3] a) F. J. Hollander, D. Coucouvanis, *Inorg. Chem.* **1974**, *13*, 2381–2386; b) M. Mitsui, H. Okawa, H. Sakiyama, M. Ohba, N. Matsumoto, T. Kurisaki, H. Wakita, *J. Chem. Soc. Dalton Trans.* **1993**, 2991–2994.
- [4] N. Kojima, W. Aoki, M. Itoi, Y. Ono, M. Seto, Y. Kobayashi, Yu. Maeda, *Solid State Commun.* **2001**, *120*, 165–170.
- [5] K. Ståhl, I. Ymén, *Acta Chem. Scand. Ser. A* **1983**, *37*, 729–737, and references therein.
- [6] E. König, *Prog. Inorg. Chem.* **1987**, *35*, 527–622; E. König, *Struct. Bonding* **1991**, *76*, 51–152.
- [7] P. Gütlich, A. Hauser, H. Spiering, *Angew. Chem.* **1994**, *106*, 2109–2141; *Angew. Chem. Int. Ed. Engl.* **1994**, *33*, 2024–2054.
- [8] O. Kahn, *Molecular Magnetism*, Wiley-VCH, New York, **1993**, chap. 4.
- [9] *Mixed-Valence Compounds* (Ed.: D. B. Brown), Reidel, Dordrecht, **1980**.
- [10] *Mixed Valency Systems: Applications in Chemistry, Physics and Biology* (Ed.: K. Prassides), Kluwer, Dordrecht, **1991**.
- [11] Y. Ogata, K. Kobayashi, T. Matsuo, H. Suga, *J. Phys. E* **1984**, *17*, 1054–1057.
- [12] Y. Kume, Y. Miyazaki, T. Matsuo, H. Suga, *J. Phys. Chem. Solids* **1992**, *53*, 1297–1304.

- [13] A. Bhattacharjee, Y. Miyazaki, M. Sorai, *J. Phys. Soc. Jpn.* **2000**, *69*, 479–488.
- [14] M. Sorai, S. Seki, *J. Phys. Soc. Jpn.* **1972**, *32*, 382–393.
- [15] P. Ganguli, V. R. Marathe, *Inorg. Chem.* **1978**, *17*, 543–550.
- [16] M. Sorai, S. Seki, *J. Phys. Chem. Solids* **1974**, *35*, 555–570.
- [17] K. Kaji, M. Sorai, *Thermochim. Acta* **1985**, *88*, 185–190.
- [18] R. D. Shannon, *Acta Crystallogr. Sect. A* **1976**, *32*, 751–767.

### Olefin Polymerization with $[\{\text{bis}(\text{imino})\text{pyridyl}\}\text{Co}^{\text{II}}\text{Cl}_2]$ : Generation of the Active Species Involves $\text{Co}^{\text{I}*}$

T. Martijn Kooistra, Quinten Knijnenburg, Jan M. M. Smits, Andrew D. Horton, Peter H. M. Budzelaar, and Anton W Gal\*

The independent discovery by the groups of Brookhart and Gibson that bis(imino)pyridyl ( $\text{N}_3$ ) complexes of iron and cobalt (Figure 1) are precursors for active polymerization and oligomerization catalysts<sup>[1]</sup> has put a new perspective on late transition metals as polymerization catalysts. However, there have been very few reports of successful extension of the system (other than trivial changes of substituents), which indicates that our understanding of this catalytic system is still incomplete.

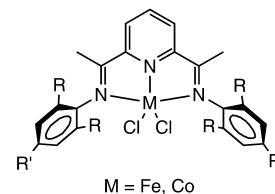


Figure 1. Previously reported bis(imino)pyridyl precatalysts  $[\text{N}_3^{\text{R}}\text{FeCl}_2]$  and  $[\text{N}_3^{\text{R}}\text{CoCl}_2]$ .<sup>[1]</sup>

The mechanism by which polymerization is believed to proceed is essentially the same as for early transition metals, that is, the active species is a cationic metal(II) alkyl complex. One recent publication contradicts this belief for the iron-based catalyst system.<sup>[2]</sup> Mechanistic studies are difficult for several reasons. In addition to problems of high activity (and hence low concentration) and the large excess of MAO (MAO = methylaluminoxane) used, the Fe and Co systems are also paramagnetic, which complicates NMR spectroscopy studies. Gibson has mentioned some preliminary studies of iron–alkyl species which appear to support formation of  $[\text{N}_3\text{FeR}]^+$ <sup>[3]</sup> moieties, but so far no reports on the corresponding Co systems have appeared. The groups of Gambarotta<sup>[4a]</sup>

[\*] Prof. Dr. A. W. Gal, T. M. Kooistra, Q. Knijnenburg, J. M. M. Smits, Dr. P. H. M. Budzelaar  
Department of Inorganic Chemistry  
University of Nijmegen  
Toernooiveld 1, 6525 ED Nijmegen (The Netherlands)  
Fax: (+31)24-355-3450  
E-mail: gal@sci.kun.nl

Dr. A. D. Horton  
Shell International Chemicals B.V.  
Shell Research and Technology Centre, Amsterdam  
P.O. Box 38000, 1030 BN Amsterdam (The Netherlands)

[\*\*] This research was sponsored by CW/STW and Basell Technology Company.